

Wearable Epilepsy Seizure Detection on FPGA with Spiking Neural Networks

Paola Busia, Gianluca Leone, Andrea Matticola, Luigi Raffo, Paolo Meloni

Abstract—The development of epilepsy monitoring solutions suitable for everyday use is a very challenging task, where different constraints should be combined, resulting from the required accuracy standards, the unobtrusiveness of the monitoring device, and the efficiency of real-time operation. Considering the time-varying nature of the electroencephalography signal (EEG), Spiking Neural Networks (SNNs) represent a promising solution to model the evolution of the brain state based on the history of the previously processed signal. This work proposes an extremely lightweight SNN-based seizure detection solution, utilizing a simple encoding scheme to ensure high levels of sparsity. Despite the reduced complexity, the model provides a detection performance comparable with the state-of-the-art SNN-based approaches on the evaluated data from the CHB-MIT dataset, reaching a 96% area under the curve (AUC) and allowing 99.3% average accuracy, with the detection of 100% of the examined seizure events and a false alarm rate of 0.3 false positives per hour. The suitability for real-time inference execution on wearable monitoring devices was assessed on SYNtzulu, demonstrating 0.5 μ s inference time with 4.55 nJ energy consumption.

Index Terms—Electroencephalography, Spiking Neural Networks, Wearable

I. INTRODUCTION

The World Health Organization estimates that 50 million individuals worldwide suffer from epilepsy, making it the most prevalent chronic brain condition [1]. People with epilepsy suffer from sudden seizure events, compromising the normal electrical activity of the brain and resulting in danger even during normal life activities. Due to this reason, both patients and caregivers have a great interest in the development and optimization of reliable remote monitoring solutions.

The standard diagnostic reference is represented by the electroencephalography (EEG) signal, which is typically analyzed by expert physicians to recognize the onset of seizure events. However, artificial intelligence approaches to automate EEG processing have been thoroughly explored in the literature, resulting in remarkable accuracy in the seizure classification [2] and seizure prediction tasks [3], but reaching adequate

This work was supported in part by Key Digital Technologies Joint Undertaking (KDT JU) in EdgeAI “Edge AI Technologies for Optimised Performance Embedded Processing” project, grant agreement No 101097300, in part by the European Union’s Horizon 2020 Research and Innovation Program under Grant Agreement GA 101140052 (H2TRAIN) and in part by NextGenerationEU Mission 4, Component 2, Investment 1.5, CUP B83C22002820006—Project METBIOTEL—Innovation Ecosystem ECS 0000024 ROME TECHNOPÔLE SPOKE 1, and SPOKE 6. Paola Busia, Gianluca Leone, Andrea Matticola, Luigi Raffo, and Paolo Meloni are with the DICE, University of Cagliari, Cagliari, Italy (e-mail: paola.busia@unica.it , gianluca.leone94@unica.it , a.matticola@studenti.unica.it , raffo@unica.it , paolo.meloni@unica.it).

standards in the low-power wearable domain is still an open research challenge.

Recently, due to the developments in neuromorphic computing, epilepsy monitoring solutions based on Spiking Neural Networks (SNNs) have been proposed, as an extremely energy-efficient approach for real-time long-term monitoring. The SNN mechanism offers an interesting opportunity to model the signal amplitude and frequency information with optimal efficiency, thanks to the inherent time-dependency in the network evolution, allowing us to consider the context of previously processed inputs. Furthermore, the binary encoding of the data removes the workload associated with multiplication execution, thus SNN inference mainly involves addition operations. Due to these reasons, SNNs represent a perfect candidate for low-power wearable monitoring solutions, which are gaining increasing interest [4]–[7].

Nonetheless, most of the spiking solutions addressing epilepsy monitoring overlook relevant issues, such as the need to reduce the acquisition setup to a low-count subset of unobtrusive channels, minimizing the stigma of a monitoring device to be used in normal life, or the need to reduce the number of false alarms, in order to improve the reliability and avoid provoking unnecessary stress to the patient. Furthermore, full utilization of the sparsity and efficiency of spiking models requires specialized neuromorphic hardware [8], [9].

In this work, we propose an extremely lightweight SNN-based epilepsy monitoring solution to address these relevant issues, by using only acquisition from the 4 temporal channels and offering a classification accuracy compatible with the detection of all the occurred seizure events, with a reduced number of false alarms. Considering accessibility as a key objective, we exploit SYNtzulu [10], a tiny low-power SNN processor design that can be squeezed on low-cost and limited-resources FPGAs such as the Lattice iCE40UP5K, which was previously considered as a target for real-time biological signal processing [11], [12]. The main contributions can be summarized as follows:

- a spiking solution for seizure detection from the raw EEG signal, leveraging a simple and effective encoding scheme and a lean SNN, ensuring the detection of 100% of the tested seizure events, with 99.3% segment-level accuracy and 0.3 false-positives-per-hour (FP/h);
- the customization of SYNtzulu’s encoding and decoding slots for the implementation of the proposed approach;
- demonstration of suitability for real-time monitoring, with inference time and power consumption measurements on the target hardware, resulting in 0.5 μ s and 4.55 nJ per inference.

The organization of the paper includes a summary of related work in literature in Section II. The proposed seizure detection approach is described in Section III, whereas the classification performance assessment is reported in Section IV-A. Section V summarizes the real-time inference performance evaluation, whereas Section VI discusses the comparison with the state-of-the-art in spiking solutions for epilepsy monitoring.

II. RELATED WORK

A comprehensive survey about SNNs for epilepsy monitoring is presented in [13], reporting works targeting seizure prediction and classification. The prediction task requires some assumptions to be made on the reference datasets, as an indication of the onset of a preictal state is often missing. For example, the authors of [14] define a 30-minute preictal interval and a prediction horizon of 5 minutes, exploiting a spiking model with 10k parameters to recognize preictal from interictal samples in the CHB-MIT dataset. In our work, we focus on the simpler classification problem, targeting the recognition of ictal samples against normal portions of the EEG recordings. The literature provides several relevant references, presenting different processing and classification solutions while targeting the same open-source dataset [15]–[21].

The authors of [15] propose an SNN model integrating three convolutional and two dense layers, applied on the Short-time Fourier Transform of one-second EEG segments, after filtering out the power line noise and the DC component. A combination of SNN and Support Vector Machine (SVM) is proposed in [16], where the execution of SNN inference is conditioned to a pre-detection mechanism based on a power threshold. The network is applied to power spectrum features, frequency-encoded into spikes considering 50 temporal steps for each new item to be classified. The energy efficiency of these solutions is assessed considering the required energy per synaptic operation on the Loihi platform [15], or the typical 50 pJ energy consumption for the emission of a spike, and 147 pJ for spike transfer on 28nm technology [16]. These approaches require the computation of Fourier transform or spectrum power prior to SNN inference, while, in our work, we consider raw EEG signals, to reduce the complexity of the processing.

A solution based on raw EEG was previously exploited in other works, such as [17], presenting a hardware implementation of a seizure detection system, exploiting level-crossing ADC applied to the raw signal and Poisson rate encoding, fed to a convolutional SNN model. Similarly, the work of [18] proposed a spiking version of the VGG network, applied on rate-coded EEG segments of 4-second length, whereas [19] presented a spiking transformer model with embedding based on temporal convolutional layers applied to 5s segments of the raw EEG signal and evaluated on both classification and prediction problems.

Despite being extremely efficient in terms of power and computational demands, the SNN models in [15]–[19] rely on complete acquisition setups, accessing 18-23 acquisition channels, designing a remarkably accurate but quite obtrusive system.

On the contrary, it is common, when focusing on wearable devices, to refer to a reduced set of electrodes. Coherently, solutions oriented to long-term monitoring outside the Epilepsy Monitoring Units (EMUs) should focus on seizure detection by accessing a limited number of acquisition channels, compatible with a reduced wearable setup, minimally impacting the normal life of the patients, and avoiding social stigma. This strict constraint is considered in recent works, such as [22] and [23], presenting a tiny transformer and a simple Convolutional Neural Network (CNN) for seizure detection based on acquisition limited to the temporal channels, and [24], proposing a self-supervised CNN evaluated based on two bipolar acquisition channels. The unobtrusiveness of the acquisition device represented a design constraint for these solutions, which demonstrated complexity and efficiency compatible with wearable monitoring devices, yet not exploiting the advantages of spiking computation.

As a direct reference for performance comparison, we consider two different works presenting SNN-based solutions leveraging access to only two acquisition channels, [20] and [21]. Both these models enable a high detection rate, leaving some room for reducing the false alarm rate, to improve the quality of user experience. With this work, we aim to improve the energy efficiency of the state-of-the-art SNN-based alternatives, with an extremely lightweight model reaching competitive detection accuracy and requiring no additional feature extraction, thanks to a simple encoding scheme capturing the most relevant EEG information and ensuring high levels of sparsity. The quantitative comparison with the alternatives from the literature is discussed in detail in Section VI.

III. METHOD

This section describes the proposed seizure detection mechanism, presenting the target dataset, as well as the encoding scheme and the network model. Finally, we include the description of the necessary modifications to SYNtzulu's architecture for real-time signal encoding, inference, and output decoding execution.

A. Dataset

The optimization and assessment of the proposed seizure detection approach targeted the open-source CHB-MIT Scalp EEG dataset [25], [26], curated by the Children's Hospital Boston and the Massachusetts Institute of Technology. The 23 pediatric patients included in the dataset presented intractable epilepsy, and were monitored during medication withdrawal. The dataset includes a list of scalp EEG records of different durations, typically one hour, annotated by experts who reported the start time and end time of seizure events. The data was collected with a 256 Hz sampling frequency, including a variable number of acquisition channels, ranging from 18 to 23.

This work targets the development of wearable systems for continuous monitoring in everyday life, we thus consider unobtrusive acquisition setups, limited to the four temporal channels compatible with behind-the-ear acquisition, namely

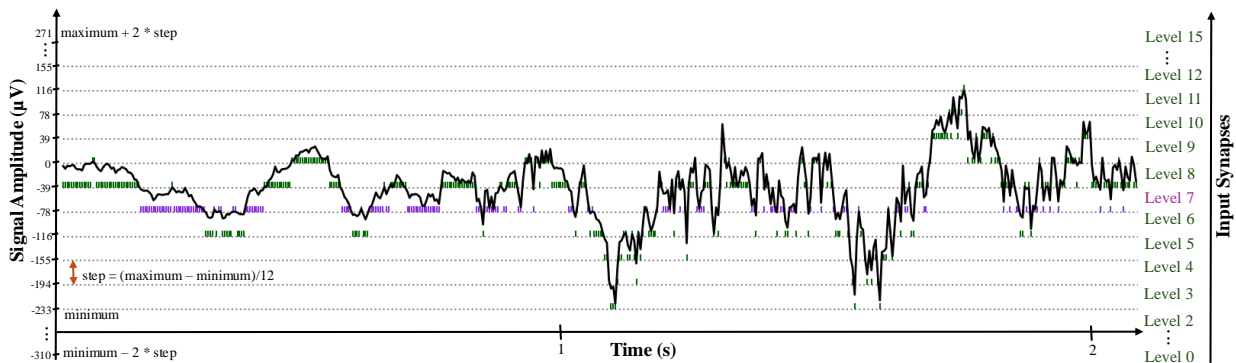


Fig. 1: Proposed encoding scheme, applied to one acquisition channel. The plot refers to an EEG excerpt from record *chb01_03*. The signal amplitude is mapped into 16 input synapses, emitting a spike when the amplitude falls within the corresponding region. A single spike is produced on one of the amplitude levels for each newly acquired sample, with a 256 Hz acquisition frequency.

TABLE I: Composition of the considered data from the CHB-MIT dataset.

Subject	Seizure records	Seizure events	Seizure time	Tested hours
chb01	7	7	7 min 22 s	6 h 40 min
chb02	3	3	2 min 52 s	2 h 15 min
chb03	7	7	6 min 42 s	7 h
chb05	5	5	9 min 18 s	5 h
chb07	3	3	5 min 25 s	9 h
chb08	5	5	15 min 19 s	5 h
chb09	3	4	4 min 36 s	9 h 30 min
chb10	7	7	7 min 27 s	14 h
chb11	3	3	13 min 26 s	2 h 50 min
Tot	43	44	1 h 12 min 27 s	61 h

F7-T7, T7-P7, F8-T8, T8-P8, according to the 10-20 international system. Based on the documented results in literature about inter-patient EEG variability [27], we focused on patient-specific epilepsy monitoring, selecting a subset of subjects including patients ranging from 1 to 11, and excluding patient *chb04*, due to a prolonged signal instability observed in record *chb04_05*, and patient *chb06*, as in [24], due to the very short duration of the seizure events recorded. No additional considerations were made for the selection of the subset of patients considered for the appropriate evaluation of the model, resulting from the order of the numbering in the dataset. Finally, considering the importance of accounting for the variability of different seizure events for the same patient, we referred to the leave-one-record-out cross-validation approach, to test the detection of seizure events completely unseen during the learning phase. For the training and test of the models, we consider only records including a seizure event. The composition of the data is summarized in Table I.

B. Encoding

EEG signal amplitude and frequency are usually especially affected by the occurrence of seizure events. Based on this consideration, we selected an encoding approach capable of highlighting the amplitude variations with time on each of the considered EEG channels, as represented in the scheme in Figure 1. The instantaneous amplitude of the signal is mapped on one of 16 different amplitude levels, defined based on the (partial) maximum and minimum value of the signal observed

during the first 5 minutes from one of the training records. The amplitude levels are equidistant, with a step defined based on the partial maximum and minimum for each channel, which are matched to levels 2 and 13, leaving four additional external representation levels for the increased signal amplitude usually observed during seizure occurrence. The amplitude of the signal acquired on each channel is thus encoded at every time step into 16 one-hot values.

Combined with the timing of the spikes, encoding the frequency-related features, this encoding scheme captures well the amplitude-related information needed for the discrimination of seizure events, as can be observed by comparing the resulting representation of normal and seizure portions of the signal, reported in Figure 2. For each acquisition channel, the plots summarize the input spike count observed on each encoding level for seizure and non-seizure windows, for one reference subject, namely *chb01*. As can be noticed, there is significant discrimination in the input spike distribution, with nonseizure windows resulting in a spiking activity limited to low-amplitude levels (central levels, from 6 to 9), and seizure windows showing noticeable activity in levels corresponding to an increased amplitude.

This intuitive encoding scheme, combined with the simplicity of the proposed classifier, provides an easily interpretable classification, based on the distribution of the input signal amplitude. It is also especially suitable for real-time implementation, as it only requires the comparison of the current amplitude value with the 16 reference levels considered. Furthermore, it enables a significant amount of sparsity in the inference computational workload, as on each temporal step only one amplitude level for each channel can receive a spike in input.

C. Network Model

The detection of seizure events on the EEG signal is performed through an extremely lightweight SNN model. The model integrates the Leaky-Integrate-and-Fire (LIF) neuron, which evolves based on the current membrane voltage value,

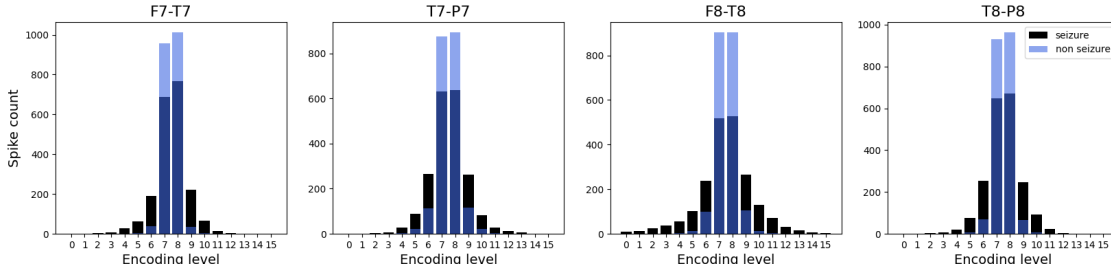


Fig. 2: Average spike count obtained for the input signal in the reference encoding levels, considering the available data from the seizure records of subject *chb01*. Spike count is evaluated on windows of 8-second length.

TABLE II: Topology and parameters of the proposed SNN model.

Layer	Synapse	Neuron	Parameters	OPS
Dense Layer 1	64	8	520	520
Dense Layer 2	8	1	9	9

$v(t)$, and based on the input current received in input, as reported in Equation 1:

$$\tilde{v}(t+1) = \alpha \cdot v(t) + \sum w \cdot s_{in}(t+1) \quad (1)$$

where $s_{in}(t+1)$ is the input train of spikes, w are the synaptic weights assigned to the input connections, and α is a decay factor. Based on the current value of the membrane voltage, the neuron produces an output spike s_{out} when a threshold value θ is reached, according to Equation 2. Finally, whenever an output spike is fired, the membrane voltage is reset by subtracting the threshold value, as reported in Equation 3.

$$s_{out}(t+1) = \begin{cases} 1, & \text{if } \tilde{v}(t+1) \geq \theta \\ 0, & \text{otherwise} \end{cases} \quad (2)$$

$$v(t+1) = \begin{cases} \tilde{v}(t+1), & \text{if } \tilde{v}(t+1) < \theta \\ \tilde{v}(t+1) - \theta, & \text{otherwise} \end{cases} \quad (3)$$

The lightweight architecture considered in this work integrates an input layer of 64 synapses, each representing the input spikes produced on each amplitude level by the signal acquired from the temporal channels. This set of input synapses is fully connected to a hidden layer including eight neurons, and finally to a single output neuron. The network architecture is summarized in Table II.

The network is trained to encode the classification between the normal and seizure classes in the firing rate of the output neuron, evaluated on a window of x temporal steps. The output rate is thus the sum of the spikes emitted by the output neuron during the x temporal steps required to process an input segment of length x . As will be detailed in Section IV.A, the typical value of x selected for training is 2048, corresponding to an input segment of length 8 s, whereas for real-time execution it is 4096.

The model's training leveraged the Pytorch framework, and particularly the SnnTorch library [28] for the LIF neuron implementation. Training is performed with backpropagation through time and aims at learning the correct output firing rate of the output neuron for each of the training segments, considering a target low rate of 0.03 for normal segments, and a target high rate of 0.35 for seizure segments. The supervised

training routine iterates over the training batches, evaluating backward propagation based on the training loss, measured as the mean squared error between the output firing rate obtained on the output neuron and the target firing rate for the target class based on the annotations on the dataset. The training is configured to complete a maximum of 500 epochs, with Adam optimizer, batch size 32, and initial learning rate 0.001. The best model is updated based on the loss evaluated on the validation set: after 20 epochs of patience where the model is not updated, the learning rate decays with a factor of 0.3. On average, training required 430 epochs. Model training was performed on Google Colaboratory.

D. Target Hardware

The proposed method has been implemented on the ultra-low-power SYNtzulu accelerator [10], shown in Figure 3. SYNtzulu is an open-source end-to-end SNN accelerator designed for tiny FPGAs¹. It efficiently processes dense spiking layers, handling 8 synapses and 2 neurons per cycle on two parallel cores, while leveraging spike sparsity. The system includes a compact bit-serial RISC-V microcontroller² that initializes the accelerator at system start-up and manages the I/O data flow through the SPI and UART modules. Moreover, the softcore gates the system when idle and automatically wakes it up when a new set of samples is available, relying on a memory-mapped timer.

The clock generation system includes both a high-frequency oscillator and a low-frequency oscillator. The only module connected to the low-frequency oscillator is the memory-mapped timer. To put the system to sleep, the processor simply turns off the high-frequency oscillator. The oscillator and the system are woken up by the timer at the appropriate time. Moreover, SYNtzulu hosts two application-specific configurable modules named *encoding* and *decoding slots*, that serve the purpose of encoding sensors' data into spikes and output spikes into the result of the classification at hand. In this work, we designed two new encoding and decoding slots to efficiently map the presented encoding and decoding algorithms in hardware.

The *encoding slot* implementation is a folded lightweight module that leverages the SPI communication latency to carry

¹<https://github.com/gianlucaleone/SYNtzulu>

²<https://github.com/olofk/serv>

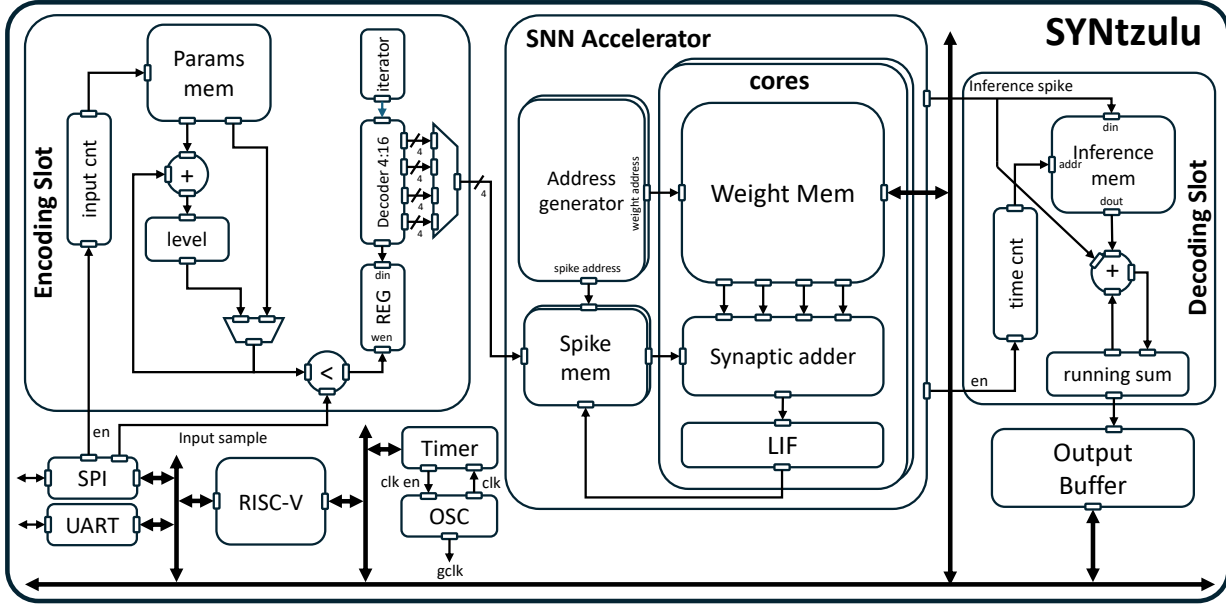


Fig. 3: SYNtulu's architecture.

out the encoding computation. The incoming samples, presented every 32 clock cycles at the input port of the encoding module, undergo a series of comparisons. A BRAM-based memory holds the minimum channel amplitude levels and the step values. Initially, the input sample is compared with the first amplitude level; if it is smaller, the amplitude level is identified; otherwise, the level is increased by the step value until the condition is satisfied. A four-bit register keeps track of the number of iterations. When the amplitude level is found, a 4 to 16 decoder generates the encoded spike set, which is then written in four entries of the SNN accelerator spike memory in four consecutive clock cycles.

The *decoding slot* computes the running sum over 4096 output inferences. To achieve this, the module incorporates a BRAM-based memory organized as 1×4096 , which stores spike values. At each network iteration, the spike count is updated according to the new spike produced by the SNN and the oldest spike discarded from the BRAM.

IV. EXPERIMENTAL RESULTS

In this section, we summarize the seizure detection results obtained in the leave-one-record-out tests of the targeted subjects, including the description of the performance assessment method and the analysis of the accuracy drop connected to the parameters' quantization.

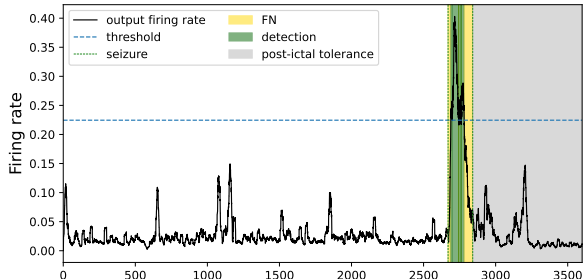
A. Classification Performance Assessment

For each subject, having N EEG records showing at least one seizure episode, we trained N different models, to be tested on the left-out record. For the training of the model, we segmented the EEG signal into windows of 8 s length, that is 2048 samples, representing x time steps. The selection of 8 s as the window length follows the findings of previous studies on real-time seizure detection [22], [27], demonstrating a higher accuracy compared to 2 s, 4 s, and 16 s

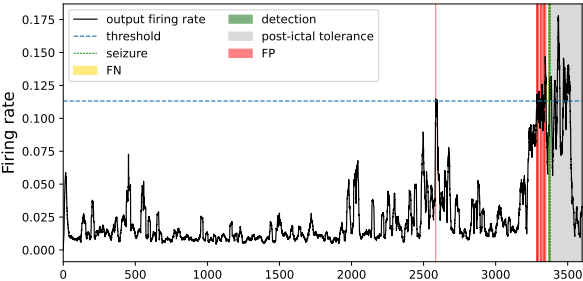
window length. A single inference run is performed to process each newly acquired sample from the temporal channels, and after 2048 steps classification is produced based on the output spike rate in the 2048 window.

While training data is randomly shuffled, for the real-time seizure detection assessment we consider the test record in chronological order, and let the network evolve for l time steps, corresponding to the whole record length. Real-time detection is evaluated for each newly acquired sample after the first x samples have been processed. The output firing rate is evaluated with a sliding window approach, referring to the $x - 1$ previous time steps, and it is compared with a patient-specific threshold to discriminate between normal and seizure segments. A common solution exploited in the literature to filter out isolated false alarms is to post-process the output with context-aware approaches, such as majority voting [22], [27]. In this work, we consider a similar solution, with the aim of reducing the impact of isolated spikes in the output rate. Instead of considering the classification output of n consecutive windows, we exploit the output firing rate definition extended to a larger segment of 4096 samples, corresponding to 16 s.

The detection results obtained are summarized in Table III. We first report the performance metrics referred to segment-level classification, considering accuracy, sensitivity, specificity, and the area under the Receiver Operating Characteristic (ROC) curve (AUC), evaluated based on their typical definition, where true positives (TP) are correctly recognized seizure segments, true negatives (TN) are correctly recognized normal segments, while false positives (FP) and false negatives (FN) are respectively mis-classifications of normal and seizure segments, and a segment is a sliding window of size x . We also include event-level metrics, considering as a TP event a seizure event detected in any portion, and as a FN event a seizure event that is not detected at all. The FP/h rate was



(a)



(b)

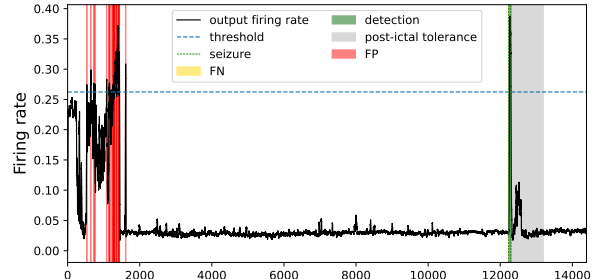
Fig. 4: Output firing rate and classification obtained executing leave-one-out inference on a) *chb08_02* and b) *chb02_19* record.

TABLE III: Classification Performance Assessment targeting the CHB-MIT dataset, considering 32-bit floating point model.

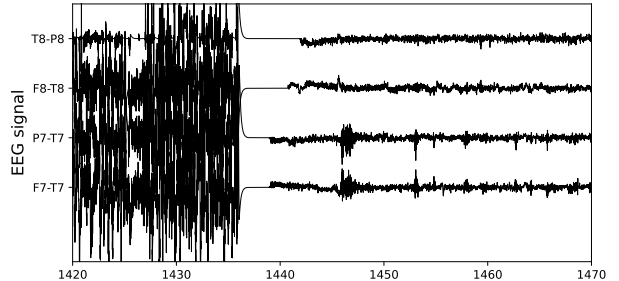
Subject	Segment-level			Event-level		
	Acc	Sens	Spec	AUC	Sens	FP/h
chb01	99.4%	68.7%	100%	97.6%	100%	0
chb02	99%	68.6%	99.7%	95.9%	100%	0.88
chb03	99.6%	76.6%	99.9%	97.7%	100%	0.14
chb05	98.8%	60.6%	100%	91.3%	100%	0
chb07	99.8%	75.1%	100%	99.6%	100%	0
chb08	98.1%	63.2%	100%	97.3%	100%	0
chb09	99%	58.8%	99.4%	96.7%	100%	1
chb10	99.7%	70.3%	99.99%	98.7%	100%	0.1
chb11	99.5%	95.4%	99.8%	98.6%	100%	0.7
Average	99.3%	72.2%	99.88%	97%	100%	0.3

obtained by considering sequences of FPs having less than 10-second distance as a single false alarm event. The maximum duration observed for an FP event is 2 minutes and 42 seconds, while the average duration is 16 seconds.

In order to display the discrimination capabilities of the model, we considered the ROC curve obtained on each of the tests performed and reported the average AUC value evaluated for each subject. As can be noticed, the AUC reaches values well beyond 90% for all of the considered subjects. The numbers in Table III refer to a working point resulting from the selection of the discrimination threshold applied to the output firing rate. The general aim is a reduction of false alarms, to improve acceptance of the monitoring device by eligible patients while ensuring the detection of all the annotated seizure events [29]–[31]. A suitable selection of the discriminating threshold was possible based on the training data and a limited 5-minute real-time observation period on



(a)



(b)

Fig. 5: a) Output firing rate and classification obtained executing leave-one-out inference on *chb09_06*. b) Detail of input EEG signal around minute 24 of *chb09_06* record.

each test record. As can be observed, accuracy numbers exceed 98% for each targeted subject, with perfect specificity in half of the subjects, and a sensitivity value ranging from 58% to 95%. We do not consider this variability to have a significant practical impact on the model's reliability, given the 100% detection rate of the evaluated seizure events. As a result, the main concern would be represented by a possible delay in the detection of the seizure. However, a certain amount of uncertainty in the onset annotation is in general to be accounted for [32]. The event-level metrics also report an average 0.3 FP/h rate, evaluated over 61 hours of the recorded signal.

Figure 4a shows an example of effective discrimination between the normal and seizure periods. The plot highlights the start time and end time of the annotated seizure. The output of the network provides an easily interpretable and explainable classification mechanism: seizure detection, highlighted in green, is obtained when the firing rate is higher than the threshold, represented by the blue horizontal line. FNs within the seizure periods are highlighted in yellow. As the EEG signal typically remains unstable for a while after seizure occurrence, we consider a tolerance period of 15 minutes, where any detection is neglected and does not result in an FP, as in [22]. A similar outcome was obtained for most of the records tested.

The FP/h metric is especially affected by the performance obtained on one of the test records for subjects *chb02* and *chb09*. Figure 4b shows the detail of the classification obtained on record *chb02_19*: as can be noticed, most of the FPs occur

TABLE IV: Classification Performance Assessment targeting the CHB-MIT dataset, considering 8-bit model.

Subject	Sample-level			Event-level		
	Acc	Sens	Spec	AUC	Sens	FP/h
chb01	99.4%	69.2%	100%	97.6%	100%	0
chb02	98.97%	66.6%	99.7%	95.9%	100%	1.3
chb03	99.5%	74%	99.9%	97.4%	100%	0.14
chb05	98.8%	60.6%	100%	91%	100%	0
chb07	99.7%	73.6%	100%	99.6%	100%	0
chb08	98.1%	62.8%	100%	97.3%	100%	0
chb09	99%	58.5%	99.4%	96.3%	100%	1
chb10	99.7%	69.5%	99.99%	98.8%	100%	0.1
chb11	99.5%	96.1%	99.8%	98.6%	100%	0.7
Average	99.3%	71.8%	99.88%	96.9%	100%	0.3

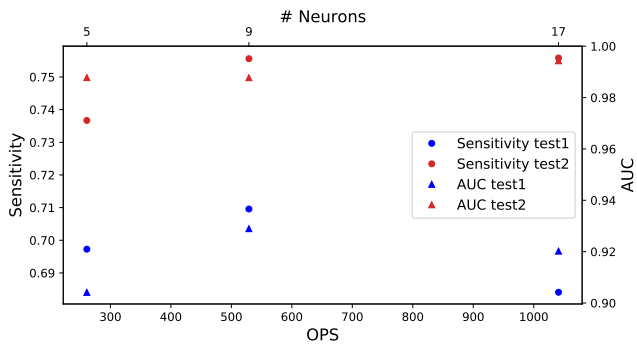


Fig. 6: Design points explored for the design of the proposed SNN model. The top x axis reports the overall neuron-count of the model, while computational requirements are reported in the bottom x axis.

a few minutes before the onset of the seizure. On the contrary, the detail of the classification output on record *chb09_06* is shown in Figure 5a, highlighting several minutes of FPs at the beginning of the record and far from the onset of the ictal event. We investigated the possible reason for this poor performance and observed an abrupt change of the EEG signal acquired compared to the first minutes of the record, as represented in Figure 5b, showing the detail of the change around minute 24. This highlights a limitation in the robustness of our proposed model. Our work does not directly tackle artifact detection, however, literature proposes solutions that can be used to assist seizure detection for this purpose, such as the use of a combined model as proposed in [33].

B. Post-Quantization Assessment

As anticipated in Section III-C, the proposed model is extremely lightweight, with only 529 parameters. Nonetheless, efficient execution on the specialized ultra-low-power accelerator targeted requires parameters' quantization to 8-bit representation. We thus repeated the classification performance assessment with the quantized model, summarizing the results in Table IV. The analysis demonstrates a limited drop in sample-level sensitivity.

C. Topology Exploration

This section analyses the design choices defining the proposed network topology. Considering the strict memory and

computational constraints resulting from the wearable deployment scenario and the interest in an easily interpretable classification outcome, we focused on a two-layer topology, including a hidden layer of processing neurons and a single output neuron, whose firing rate provides the final classification.

To assess the optimality of the proposed topology in Table II, we include in the following the results of a design exploration on the width of the hidden layer, summarized in Figure 6. The evaluated design points exploit a number of hidden neurons selected from the set {4, 8, 16}. The plot reports the sensitivity and AUC obtained on two different tests performed on seizure records from patient 1 of the CHB-MIT dataset. The results of both tests, reported in different colors, demonstrate the drop in the seizure detection performance resulting from reducing the number of hidden neurons below 8. On the contrary, the advantages of further increasing it to 16 are not consistent, as can be observed based on the results of test 1, despite a factor 2× increase in the computational requirements. The candidate 9-neurons topology was thus selected for the study, considering the advantages in terms of required inference time and energy consumption in real-time.

D. Seizure Detection Generalization

Using other datasets to assess the generality of the methods is not straightforward, as alternative datasets use other data collection and partitioning approaches that do not match well our training strategy. For example, the Temple University Hospital EEG Seizure Corpus (TUSZ) [34], [35] reports much shorter tracks with limited non-ictal sections. On the other hand, our approach relies on more data for training. This is easily achievable, in real life, with long patient-specific recording and monitoring sessions, as in CHB-MIT. Despite these unfavorable conditions, we tested our approach on different sources, to generally assess the capability of the encoding approach and of the network to discriminate seizures. We thus applied the presented training and classification process to two additional open-source epilepsy datasets, the TUSZ dataset and the Bonn dataset [36].

The TUSZ dataset reports EEG recordings and seizure annotations for several subjects, acquired at varying sampling frequencies, e.g. 250 Hz and 400 Hz. For the assessment described in the following, we considered 6 of the available subjects selected based on two main criteria: 1) having at least three seizure records, providing at least two independent seizure examples for training, and one for a leave-one-out test; 2) presenting a suitable balance between the available normal and seizure data, and no prevalence of records reporting extremely frequent and short seizures. These criteria match the practical application scenario we imagine for the proposed system, trained in a subject-specific manner on a given amount of normal and seizure recordings.

As we did on the CHB-MIT dataset, we only considered the information acquirable through the 4 temporal channels, resampled to a common 250 Hz frequency. We performed 6 independent trainings and tested the models on a left-out

TABLE V: Assessment of subject-specific seizure detection performance on the TUSZ dataset.

Subject	Sample-level				Event-level	
	Acc	Sens	Spec	AUC	Sens	FP/h
aaaaaac	94.94%	92.4%	100%	98%	100%	0
aaaaaalq	48.29%	34.73%	93.5%	65%	100%	0.02
aaaaabms	90.96%	43.69%	100%	68%	100%	0
aaaaabnn	62.22%	7 %	100%	89%	100%	0
aaaaadno	74%	27.3%	100%	84%	100%	0
aaaaadpj	75.77%	67.1%	100%	84%	100%	0
Average	62.4%	41.9%	97.8%		100%	0.01

seizure record. The results of the assessment are summarized in Table V. As can be observed, the proposed method enables the detection of 100% of the annotated seizure events in the records tested, despite a segment-level accuracy and sensitivity demonstrating values below those obtained on the CHB-MIT dataset. Due to the shorter duration of the test records, the postictal tolerance was reduced to only 60 seconds, nonetheless, perfect specificity was obtained on most of the tests. The proposed model can thus be applied successfully for the EEG monitoring of diverse patients, even if reaching different classification performance based on the subject and the available data.

The second reference resource is the Bonn dataset, collecting five subsets of single-channel EEG data acquired with surface or intracranial setups: subsets A and B include recordings from healthy subjects, with eyes open or closed; subsets C and D include recordings of epileptic patients during seizure-free activity, whereas set E includes recordings of seizure events. Each subset includes 100 segments of 23.6 s duration, acquired with 173.61 Hz sampling frequency and stored in separate records.

For the assessment of our proposed model, we considered subsets C, D, and E, related to the epilepsy monitoring problem, enforcing a 70:10:20 training-validation-test split on each subset to ensure the isolation of the test set, which thus includes 20 segments from subset E, labeled as normal, 20 segments from subset F, labeled as normal, and 20 segments from subset E, labeled as seizure. The organization of the data per subject, in fact, is not disclosed. The considered topology only differs from the one summarized in Table II because of the number of input synapses in the first layer, reduced to 16 due to the single channel data acquisition. The test of the trained model, after 300 epochs of training, demonstrated a classification accuracy of 92.6%, with segment-level sensitivity and specificity of respectively 78.9% and 100%. An event-level sensitivity of 95% was evaluated considering the 20 recordings from subset E as 20 distinct seizure events. The summary of the detection performance is reported in Figure 7, reporting the output firing rate throughout the set, and the discriminating threshold selected based on the training data. As can be observed, the test set was organized with the seizure records at the end of the set. Successful detection is highlighted in green, whereas missed detection is indicated in yellow. Overall, the assessment on the Bonn dataset demonstrated promising generalization capabilities, with 0 FP/h observed.

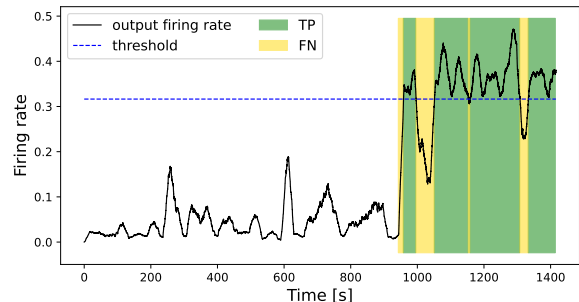


Fig. 7: Output firing rate and classification obtained on the Bonn dataset, for 70:10:20 training-validation-test split.

V. DEPLOYMENT

This section summarizes the key hardware performance figures evaluated considering real-time inference execution on the SYNtzulu hardware target, including sparsity evaluation and inference time and power consumption measurements.

A. Implementation

The design has been implemented on the Lattice iCE40UP5K FPGA, a tiny computing canvas that counts 5,280 logic cells (LCs) composed of one LUT and one FF, 8 DSPs including a 16x16 bit multiplier and a 32-bit accumulator, 30 4-kb dual-port block RAMs (BRAMs), and 4 256-kb single-port RAMs (SPRAMs). The FPGA also embeds two oscillators; the former can generate a low-frequency clock of 10 kHz, and the latter can be configured to work at 24, 12, 8, or 4 MHz.

The resource requirements for our implementation are summarized in Table VI.

TABLE VI: Resource requirements of SYNtzulu on the Lattice iCE40UP5K FPGA.

	LC	DSP	BRAM	SPRAM
System	3271 (61%)	2 (25%)	14 (46%)	4 (100%)
Encoding	163 (3.0%)	0 (0%)	1 (3.3%)	0 (0%)
Decoding	85 (1.6%)	0 (0%)	1 (3.3%)	0 (0%)

B. Sparsity

One of the key advantages of spiking computation, along with the possibility of replacing multiplications with additions, is the sparsity introduced by the binary encoding of network spikes, allowing computations to be executed only when an input spike is received. To assess the typical workload of inference execution based on our proposed model, we evaluated the percentage of active spikes resulting on average from the processing of the test data, which is only 7.3%. This result is aligned with expectations based on the selected encoding scheme, as only 1/16 of the input synapses can spike at each given time step. This maximum theoretical gain resulting from the nature of the input data, of 92.7%, can be defined as *software sparsity*.

To what extent this amount of sparsity can be exploited in terms of efficiency gain depends on how well sparse

TABLE VII: Inference time and core power consumption on SYNtzulu.

Energy component	Power consumption	Time
Inference (P_{inf} , T_{inf})	9.1 mW	0.5 μ s
Idle (P_{idle} , T_{idle})	0.25 mW	3.89 ms

computations can be mapped on the target hardware. In the case of SYNtzulu [10], the integration of 4 adjacent synapses is executed in parallel. Therefore, we also evaluated the available *hardware sparsity*, considering at each time step the organization of the input synapses into groups of 4, and accounting for a contribution of 4 active spikes to the computations performed whenever the group includes at least one active spike. With this constraint, the percentage of average active operations grows to 17.2%, resulting in a *hardware sparsity* of 82.8%. This value resulted from the average count of active quartets of spikes monitored through dedicated counters during inference on the test set. The organization of consecutive spikes in quartets emulated the scheduling of computations performed in hardware. For each active quartet, a contribution of 4 active spikes was considered.

C. Real-time Inference Performance

When the monitoring device is working in real-time, a new classification output will be produced in a streaming manner with a single inference run, after the first window of size 4096 considered for the firing rate computation is fully computed. As anticipated in Table II, the execution of one inference run on a newly acquired set of synapses at a given time step requires 529 accumulate OPS, which rounds up to 556 OPS due to the size of the parallelism on the target platform. This number represents the higher bound of required operations, as on average, due to the available sparsity, only 96 OPS per inference need to be performed.

The on-hardware performance evaluated on SYNtzulu, obtained according to the methodology described in [10] and considering 24 MHz working frequency, is reported in Table VII. The table refers to an inference execution frequency of 256 Hz, based on the sampling frequency of the EEG data from the CHB-MIT dataset. The resulting core power profile is reported in Figure 8, demonstrating a core energy consumption per inference of 4.55 nJ, given an average inference execution time of 0.5 μ s. The measurement setup is shown in Figure 9.

To minimize the energy/resource cost of the encoding, the encoding module is designed to complete an encoding of a newly acquired signal sample during its SPI signal acquisition. Once the spikes on the 4 channels are obtained, the SNN inference is evaluated. Its active time is minimized by exploiting sparsity at best, except for the waste in parallel exploitation quantified as *hardware sparsity*. Communication-related efficiency is also improved, by setting the host processor to only transmit an output alert when a seizure is detected, thus making the output transmission payload negligible. Therefore, in-place processing enables a dramatic reduction of required communication bandwidth, with respect to an acquisition system transmitting raw data, requiring 16 kB/s for 4 channels, sampled at 256 Hz frequency with 16-bit precision.

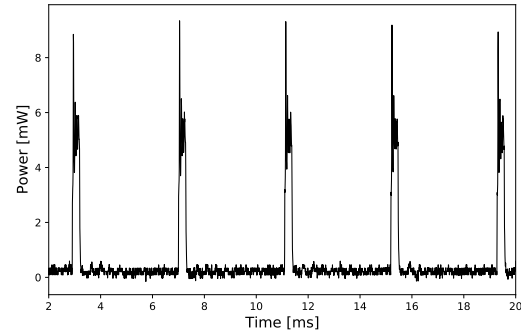


Fig. 8: Real-time core power consumption on SYNtzulu.

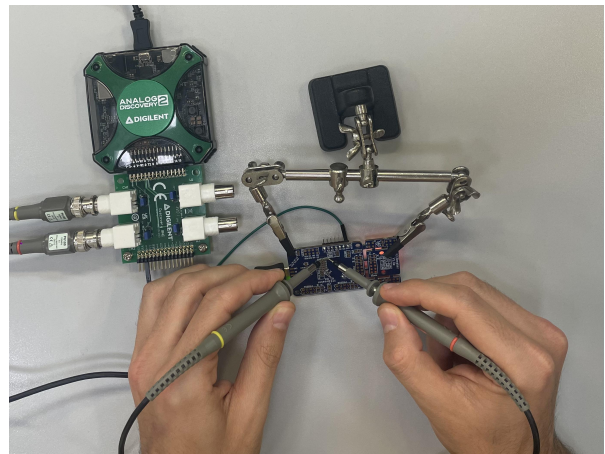


Fig. 9: Power measurement setup.

VI. DISCUSSION

Table VIII reports the comparison with the seizure detection performance achieved on the CHB-MIT dataset by SNN approaches from the state of the art. As a first general consideration, the listed works target seizure detection based on different acquisition setups, ranging from full montage [15]–[19], to unobtrusive minimal setups [20], [21]. The signs of seizure occurrence can be detected more easily with access to full acquisition setups, as is demonstrated by the excellent performance achieved especially in [18] and [19], showcasing 95% sensitivity with over 99% specificity, however, similar monitoring devices would not be suitable for continuous monitoring outside the EMUs, where more unobtrusive solutions should be favored. Nonetheless, despite the constraints on the acquisition setup, our seizure detection system surpasses the solution in [15], providing an improved specificity compared to [16] and [17], based on the tests performed.

Additionally, the referenced works select different trade-offs between the sensitivity and specificity of the detection. Our choice results from the need to ensure as low a number of false alarms as possible, while enabling the detection of 100% of the seizure events, as this balance is crucial for the practical use of a monitoring device [29]–[31]. From this perspective, the leave-one-record-out test approach we considered closely resembles the real-time practical scenario,

TABLE VIII: Seizure detection based on SNNs on the CHB-MIT dataset.

Model	Channels	Features	Segment-level			Event-level		OPS	Memory
			Sens	Spec	AUC	Sens	FP/h		
[15]	22	STFT	N.R.	N.R.	90.5%	N.R.	N.R.	304 k ***	484 kB ***
[16]	23	power spectrum	88.4%	84.6%	N.R.	N.R.	N.R.	6 k **	14 kB ***
[17]	23	raw	92.2%	97.3%	N.R. *	100%	N.R.	1.5 - 0.2 M **	9.75 kB
[18]	22	raw	95.06%	99.45%	N.R.	N.R.	N.R.	58.4 M ***	N.R.
[19]	22	raw	94.9%	99.3%	N.R.	N.R.	N.R.	0.32 M	9.9 kB
[20]	2	raw filtered	90.4%	96.7%	N.R.	N.R.	N.R.	N.R.	2.4 kB
[21]	2	raw	78.7%	76.9%	N.R.	N.R.	N.R.	57 k **	69 kB ***
this	4	raw	71.8%	99.88%	96.9%	100%	0.3	529	529 B

* Not Reported.

** Accounting for observed sparsity.

*** Estimated from the paper.

where a model is trained on a set of seizure events and then is asked to recognize independent ones, that have not been seen in any portion during the learning phase, resulting in a lower classification accuracy than the one achievable if the chronological separation between training and test seizure events is not ensured.

Despite the possible differences resulting from the test approach, the comparison with the two works leveraging a reduced acquisition setup [20], [21] suggests our model provides a higher specificity level, which does not hinder the ability of the monitoring system to detect all the evaluated seizure events. However, to enable a more direct comparison of the achievable performance with the results documented in the literature, we considered the ROC curve of our proposed model and evaluated the classification metrics resulting from a subset of working points with comparable specificity. With a threshold selection resulting in 97.3% average specificity, as reported in [17], the sensitivity of our model increases to 87.1%, and up to 88.2% when the specificity is 96.7%, as in [20]. Lastly, further reducing the specificity to 84.6%, such as in [16], the resulting sensitivity is 96%.

Finally, a clear advantage of our proposed approach, highlighted by the analysis in the Table, is a significant reduction of the required number of operations per inference and of the memory requirements for the storage of the network parameters. For all of the listed works, we assumed 8-bit representation whenever not explicitly stated differently.

VII. CONCLUSIONS

In this work, we presented an efficient spiking solution for epilepsy monitoring in everyday life, considering the constraints resulting from the necessary unobtrusiveness of a similar device. We designed an encoding scheme aiming at capturing the signal frequency and amplitude information without the need for complex feature extraction and combined it with a lean SNN model performing classification between normal and seizure segments based on the firing rate of the output neuron. The assessment on the open-source CHB-MIT dataset shows a 96% AUC, enabling a 100% seizure event detection rate in the considered subjects, with a limited 0.3 FP/h rate, which is competitive with the alternative SNN-based approaches evaluated on reduced acquisition setups. Furthermore, the computational complexity is significantly reduced, with only 96 accumulate operations required on average for a new classification, resulting in 0.5 μ s and 4.55 nJ core

energy consumption per inference. This analysis thus provides significant advancements in the EEG long-term monitoring problem, creating a solid base for further improvements in the generalization capabilities and the reduction of false alarms, to encourage final practical use.

ACKNOWLEDGMENT

REFERENCES

- [1] W. H. Organization. Epilepsy. [Online]. Available: <https://www.who.int/news-room/fact-sheets/detail/epilepsy>
- [2] M. Sahani, S. K. Rout, and P. K. Dash, "Epileptic seizure recognition using reduced deep convolutional stack autoencoder and improved kernel rvfln from eeg signals," *IEEE Transactions on Biomedical Circuits and Systems*, vol. 15, no. 3, pp. 595–605, 2021.
- [3] R. Zhu, W.-x. Pan, J.-x. Liu, and J.-l. Shang, "Epileptic seizure prediction via multidimensional transformer and recurrent neural network fusion," *Journal of Translational Medicine*, vol. 22, p. 895, 2024.
- [4] S. Frey, M. A. Lucchini, V. Kartsch, T. M. Ingolfsson, A. H. Bernardi, M. Segesssenmann, J. Osieleniec, S. Benatti, L. Benini, and A. Cossettini, "Gapses: Versatile smart glasses for comfortable and fully-dry acquisition and parallel ultra-low-power processing of eeg and eog," *IEEE Transactions on Biomedical Circuits and Systems*, pp. 1–11, 2024.
- [5] D. Sopic, A. Aminifar, and D. Atienza, "e-glass: A wearable system for real-time detection of epileptic seizures," *2018 IEEE International Symposium on Circuits and Systems (ISCAS)*, pp. 1–5, 2018.
- [6] M. Guermandi, S. Benatti, V. J. Kartsch Morinigo, and L. Bertini, "A wearable device for minimally-invasive behind-the-ear eeg and evoked potentials," *2018 IEEE Biomedical Circuits and Systems Conference (BioCAS)*, pp. 1–4, 2018.
- [7] N. Pham, T. Dinh, Z. Raghebi, T. Kim, N. Bui, P. Nguyen, H. Truong, F. Banaei-Kashani, A. Halbower, T. Dinh, and T. Vu, "Wake: A behind-the-ear wearable system for microsleep detection," *Association for Computing Machinery*, p. 404–418, 2020. [Online]. Available: <https://doi.org/10.1145/3386901.3389032>
- [8] G. Orchard, E. P. Frady, D. B. D. Rubin, S. Sanborn, S. B. Shrestha, F. T. Sommer, and M. Davies, "Efficient neuromorphic signal processing with loihi 2," in *2021 IEEE Workshop on Signal Processing Systems (SiPS)*, 2021, pp. 254–259.
- [9] M. V. DeBole, B. Taba, A. Amir, F. Akopyan, A. Andreopoulos, W. P. Risk, J. Kusnitz, C. Ortega Otero, T. K. Nayak, R. Appuswamy, P. J. Carlson, A. S. Cassidy, P. Datta, S. K. Esser, G. J. Garreau, K. L. Holland, S. Lekuch, M. Mastro, J. McKinstry, C. di Nolfo, B. Paulovicks, J. Sawada, K. Schleupen, B. G. Shaw, J. L. Klamo, M. D. Flickner, J. V. Arthur, and D. S. Modha, "Truenorth: Accelerating from zero to 64 million neurons in 10 years," *Computer*, vol. 52, no. 5, pp. 20–29, 2019.
- [10] G. Leone, M. Antonio Scrugli, L. Badas, L. Martis, L. Raffo, and P. Meloni, "Syntzulu: A tiny risc-v-controlled snn processor for real-time sensor data analysis on low-power fpgas," *IEEE Transactions on Circuits and Systems I: Regular Papers*, vol. 72, no. 2, pp. 790–801, 2025.
- [11] M. A. Scrugli, P. Busia, G. Leone, and P. Meloni, "On-fpga spiking neural networks for integrated near-sensor ecg analysis," in *2024 Design, Automation Test in Europe Conference Exhibition (DATE)*, 2024, pp. 1–6.

- [12] M. A. Scrugli, G. Leone, P. Busia, L. Raffo, and P. Meloni, "Real-time semg processing with spiking neural networks on a low-power 5k-lut fpga," *IEEE Transactions on Biomedical Circuits and Systems*, vol. 19, no. 1, pp. 68–81, 2025.
- [13] R. Cherian and G. M. Kanaga E, "Unleashing the potential of spiking neural networks for epileptic seizure detection: A comprehensive review," *Neurocomputing*, vol. 598, p. 127934, 2024. [Online]. Available: <https://www.sciencedirect.com/science/article/pii/S0925231224007057>
- [14] F. Tian, J. Yang, S. Zhao, and M. Sawan, "A new neuromorphic computing approach for epileptic seizure prediction," in *2021 IEEE International Symposium on Circuits and Systems (ISCAS)*, 2021, pp. 1–5.
- [15] Y. Yang, J. K. Eshraghian, N. Duy Truong, A. Nikpour, and O. Kavehei, "Neuromorphic deep spiking neural networks for seizure detection," *Neuromorphic Computing and Engineering*, vol. 3, no. 1, p. 014010, feb 2023. [Online]. Available: <https://dx.doi.org/10.1088/2634-4386/acbab8>
- [16] H. Shan, L. Feng, Y. Zhang, L. Yang, and Z. Zhu, "Compact seizure detection based on spiking neural networks and support vector machine for efficient neuromorphic implementation," *Biomedical Signal Processing and Control*, vol. 86, p. 105268, 2023. [Online]. Available: <https://www.sciencedirect.com/science/article/pii/S1746809423007012>
- [17] A. Muneeb and H. Kassiri, "Customized development and hardware optimization of a fully-spiking snn for eeg-based seizure detection," in *2024 IEEE Biomedical Circuits and Systems Conference (BioCAS)*, 2024, pp. 1–5.
- [18] A. Javanshir, T. T. Nguyen, M. A. Parvez Mahmud, and A. Z. Kouzani, "A deep convolutional spiking neural network for embedded applications," *Progress in Artificial Intelligence*, vol. 13, pp. 1–15, 2024.
- [19] Q. Chen, C. Sun, C. Gao, and S.-C. Liu, "Epilepsy seizure detection and prediction using an approximate spiking convolutional transformer," in *2024 IEEE International Symposium on Circuits and Systems (ISCAS)*, 2024, pp. 1–5.
- [20] R. Li, G. Zhao, D. R. Muir, Y. Ling, K. Burelo, M. Khoe, D. Wang, Y. Xing, and N. Qiao, "Real-time sub-milliwatt epilepsy detection implemented on a spiking neural network edge inference processor," *Computers in Biology and Medicine*, vol. 183, p. 109225, 2024. [Online]. Available: <https://www.sciencedirect.com/science/article/pii/S0010482524013106>
- [21] X. Erickson, S. Bastani, and A. Aminifar, "Personalized seizure detection using spiking neural networks," in *2023 IEEE International Conference on Omni-layer Intelligent Systems (COINS)*, 2023, pp. 1–6.
- [22] P. Busia, A. Cossettini, T. M. Ingolfsson, S. Benatti, A. Burrello, V. J. B. Jung, M. Scherer, M. A. Scrugli, A. Bernini, P. Ducouret, P. Ryvlin, P. Meloni, and L. Benini, "Reducing false alarms in wearable seizure detection with eegformer: A compact transformer model for mcus," *IEEE Transactions on Biomedical Circuits and Systems*, vol. 18, no. 3, pp. 608–621, 2024.
- [23] T. M. Ingolfsson, X. Wang, U. Chakraborty, S. Benatti, A. Bernini, P. Ducouret, P. Ryvlin, S. Beniczky, L. Benini, and A. Cossettini, "Brainfusenet: Enhancing wearable seizure detection through eeg-ppg-accelerometer sensor fusion and efficient edge deployment," *IEEE Transactions on Biomedical Circuits and Systems*, vol. 18, no. 4, pp. 720–733, 2024.
- [24] B. Huang, R. Zanetti, A. Abtahi, D. Atienza, and A. Aminifar, "Epilepsynet: Interpretable self-supervised seizure detection for low-power wearable systems," in *2023 IEEE 5th International Conference on Artificial Intelligence Circuits and Systems (AICAS)*, 2023, pp. 1–5.
- [25] A. H. Shoeb, "Application of machine learning to epileptic seizure onset detection and treatment," *Ph.D. dissertation, MIT*, 2009.
- [26] A. L. Goldberger *et al.*, "Physiobank, physiotoolkit, and physionet: components of a new research resource for complex physiologic signals," *circulation*, vol. 101, pp. e215–e220, 2000.
- [27] T. M. Ingolfsson, A. Cossettini, X. Wang, E. Tabanelli, G. Tagliavini, P. Ryvlin, L. Benini, and S. Benatti, "Towards long-term non-invasive monitoring for epilepsy via wearable eeg devices," in *2021 IEEE Biomedical Circuits and Systems Conference (BioCAS)*, 2021, pp. 01–04.
- [28] J. K. Eshraghian, M. Ward, E. Neftci, X. Wang, G. Lenz, G. Dwivedi, M. Bennamoun, D. S. Jeong, and W. D. Lu, "Training spiking neural networks using lessons from deep learning," *Proceedings of the IEEE*, vol. 111, no. 9, pp. 1016–1054, 2023.
- [29] E. Bruno, P. F. Viana, M. R. Sperling, and M. P. Richardson, "Seizure detection at home: Do devices on the market match the needs of people living with epilepsy and their caregivers?" *Epilepsia*, vol. 61, pp. S11–S24, 2020.
- [30] C. Baumgartner and J. P. Koren, "Seizure detection using scalp-eeg," *Epilepsia*, vol. 59, no. S1, pp. 14–22, 2018.
- [31] A. Van de Vel, K. Smets, K. Wouters, and B. Ceulemans, "Automated non-eeg based seizure detection: Do users have a say?" *Epilepsy & Behavior*, vol. 62, pp. 121–128, 2016. [Online]. Available: <https://www.sciencedirect.com/science/article/pii/S1525505016302141>
- [32] J. Dan, U. Pale, A. Amirshahi, W. Cappelletti, T. M. Ingolfsson, X. Wang, A. Cossettini, A. Bernini, L. Benini, S. Beniczky, D. Atienza, and P. Ryvlin, "Szscore: Seizure community open-source research evaluation framework for the validation of electroencephalography-based automated seizure detection algorithms," *Epilepsia*, vol. n/a, no. n/a. [Online]. Available: <https://onlinelibrary.wiley.com/doi/abs/10.1111/epi.18113>
- [33] T. M. Ingolfsson, S. Benatti, X. Wang, A. Bernini, P. Ducouret, P. Ryvlin, S. Beniczky, L. Benini, and A. Cossettini, "Minimizing artifact-induced false-alarms for seizure detection in wearable eeg devices with gradient-boosted tree classifiers," *Scientific Reports*, vol. 14, p. 2980, 2024. [Online]. Available: <https://doi.org/10.1038/s41598-024-52551-0>
- [34] I. Obeid and J. Picone, "The temple university hospital eeg data corpus," *Frontiers in Neuroscience*, vol. Volume 10 - 2016, 2016. [Online]. Available: <https://www.frontiersin.org/journals/neuroscience/articles/10.3389/fnins.2016.00196>
- [35] V. Shah, E. von Weltin, S. Lopez, J. R. McHugh, L. Veloso, M. Golmohammadi, I. Obeid, and J. Picone, "The temple university hospital seizure detection corpus," *Frontiers in Neuroinformatics*, vol. Volume 12 - 2018, 2018. [Online]. Available: <https://www.frontiersin.org/journals/neuroinformatics/articles/10.3389/fninf.2018.00083>
- [36] R. G. Andrzejak, K. Lehnertz, F. Mormann, C. Rieke, P. David, and C. E. Elger, "Indications of nonlinear deterministic and finite-dimensional structures in time series of brain electrical activity: Dependence on recording region and brain state," *Phys. Rev. E*, vol. 64, p. 061907, Nov 2001. [Online]. Available: <https://link.aps.org/doi/10.1103/PhysRevE.64.061907>